Theoretical Studies of Inorganic and Organometallic Reaction Mechanisms. 3. The Origin of the Difference in the Barrier for the Kinetic and Thermodynamic Products for the Oxidative Addition of Dihydrogen to a Square-Planar Iridium Complex

Andrew L. Sargent,[†] Michael B. Hall,*[,†] and Martyn F. Guest[‡]

Contribution from the Department of Chemistry, Texas A&M University, College Station, Texas 77843-3255, and SERC Daresbury Laboratory, Warrington, WA4, 4AD, U.K.
Received April 30, 1991

Abstract: The stereoselective oxidative addition of H_2 to IrCl(CO)(dppe) was examined with ab initio theoretical techniques. Reaction coordinates for the two pathways to addition which lead to the formation of the two isomers were constructed from geometry optimization calculations and were augmented by significant portions of the potential energy surfaces near the transition states. The analysis of the Laplacian of the total charge densities revealed that as the complexes evolve from four-coordinate to six-coordinate species, the ligands in the plane of addition move past regions of charge concentration around the metal center. Electron-withdrawing ligands in the plane of addition reduce this repulsive interaction by delocalizing a portion of the electronic charge. Electron-donor ligands are unable to function in this capacity and therefore contribute to the repulsive interaction of the five-coordinate transition state to a greater extent. The influence of electron correlation on the reaction coordinates was examined and found not to significantly alter the conclusions based on the single-determinant calculations.

Introduction

The oxidative addition of H_2 to transition-metal complexes is an important step in catalytic hydrogenation and hydroformylation processes.[1] In d^8 square-planar transition-metal complexes where the symmetry is neither C_{2v} nor D_{4h}, the concerted addition of H_2 yields two possible structural isomers, depending along which diagonal ligand axis of the square-planar complex the H_2 unit adds (Scheme I). The study of the factors which control the direction of addition, and hence the stereochemistry of the final product, has been a complicated task due to the competing steric and electronic effects among the ligands in the square-planar complex.

The interest in this area has been renewed, however, due to the recent report by Eisenberg and co-workers on the oxidative addition of H_2 to IrCl(CO)(dppe) (dppe = 1,2-bis(diphenylphosphino)ethane).[2] The two principal features that are responsible for the renewed interest are as follows. First, the steric and electronic effects from the phosphine ligands on the direction of addition essentially cancel since one phosphine ligand is present in both planes of addition. Second, the isomer which is formed as a result of addition along the P-Ir-CO axis is formed with greater than 99% stereoselectivity at low temperatures, while the other isomer, formed from the addition along the P-Ir-Cl axis, appears at higher temperatures and eventually dominates the final equilibrium (Scheme II). That the relative stabilities of the transition states along the reaction paths are not simply a consequence of the stabilities of the final products indicates that a unique factor is at work in the early stages of the reaction to determine the direction of addition. Due to the cancellation of the influence from the phosphine ligands, this factor is likely due to the steric and/or electronic difference between the CO and Cl ligands.

Early theoretical work on a simplified rhodium model suggested that addition in the P-Rh-CO plane was favored as a result of a stabilizing backbonding interaction between the metal and the carbonyl ligand in the five-coordinate transition state.[3] A similar type of stabilization due to the trans effect[4] of strong π-accepting ligands was recently analyzed in a substitution reaction at square-planar platinum(II) and rhodium(I) complexes.[5] The generalization of these results that the addition of H_2 to any d^8 square-planar transition-metal complex would proceed in the plane of the strongest π-acceptor ligand proved invalid, as shown by Crabtree and co-workers.[6] This work suggested that the influence of the other ligands on the stability of the transition state cannot be neglected. Thus, we have undertaken a more accurate theoretical analysis of the oxidative addition of H_2 to IrCl(CO)(dppe), paying particular attention to the influence of the Cl ligand on the stability of the five-coordinate transition state.

Methods

Reaction coordinates for the oxidative addition of H_2 to IrCl(CO)(dppe) were constructed from a series of full gradient[7] geometry optimizations of the model **1** at the restricted Hartree-Fock-Roothaan (HFR) level of theory.[8] The variable of the reaction coordinate, r, which

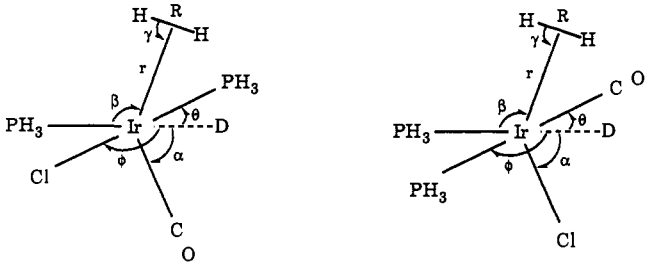

1

defined the distance from the metal atom to the centroid of the H_2 unit, was fixed at several values while other geometric parameters were varied. In the model, D was a dummy atom used to define three of the five angular degrees of freedom allowed in the optimizations. It was oriented collinear with the Ir-PH_3 unit. All metal-ligand bond distances as well as the C-O and H-H distances were also allowed to vary. The dppe ligand was replaced by two PH_3 groups, and the Ir-PH_3 bond distances were constrained to be equal, since the crystal structure of IrBr(CO)-

[†] Texas A&M University.
[‡] S.E.R.C. Daresbury Laboratory.

(1) (a) Cotton, F. A.; Wilkinson, G. *Advanced Inorganic Chemistry, 5th ed.*; Wiley: New York, 1988; p 1186. (b) Parshall, G. W. *Homogenous Catalysis*; Wiley: New York, 1980.
(2) (a) Fisher, B. J.; Eisenberg, R. *Inorg. Chem.* **1984**, *23*, 3216. (b) Johnson, C. E.; Fisher, B. J.; Eisenberg, R. *J. Am. Chem. Soc.* **1983**, *105*, 7772. (c) Johnson, C. E.; Eisenberg, R. *J. Am. Chem. Soc.* **1985**, *107*, 3148. (d) Johnson, C. E.; Eisenberg, R. *J. Am. Chem. Soc.* **1985**, *107*, 6531.
(3) (a) Jean, Y.; Lledos, A. *Nouv. J. Chim.* **1986**, *10*, 635. (b) Halpin, C. F. Masters Thesis; Texas A&M University, College Station, TX, 1986.
(4) Cotton, F. A.; Wilkinson, G. *Advanced Inorganic Chemistry*, 5th ed.; Wiley: New York, 1988; pp 1299-1300.
(5) Lin, Z.; Hall, M. B. *Inorg. Chem.* **1991**, *30*, 646.
(6) Burk, M. J.; McGrath, M. P.; Wheeler, R.; Crabtree, R. H. *J. Am. Chem. Soc.* **1988**, *110*, 5034.
(7) Pulay, P. *Mol. Phys.* **1969**, *17*, 197.
(8) Roothaan, C. C. J. *Rev. Mod. Phys.* **1951**, *23*, 69.

0002-7863/92/1514-517$03.00/0

Scheme I

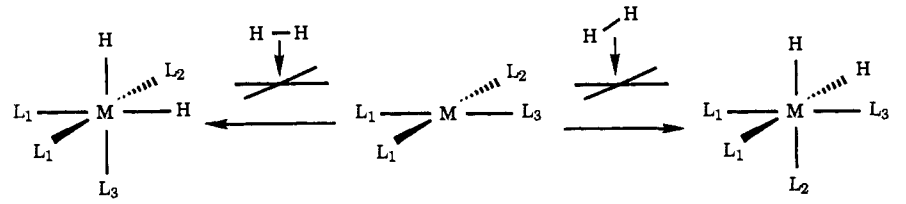

Scheme II

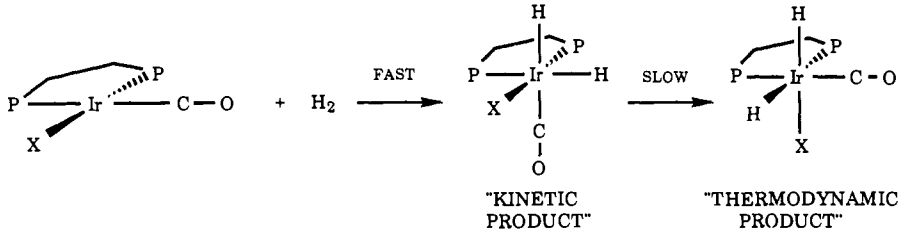

(dppe) showed that these M–P distances varied by only 0.02 Å despite the large electronic differences in the ligands that were trans to these bonds.[2c]

The ECP2-type pseudopotential basis set[9a] for Ir was chosen over the ECP1-type basis[9b] in deference to other studies[10,11] which weighed the relative merits of both ECP1- and ECP2-type sets. With the ECP2-type basis, the outer core electrons (the $5s^2$ and $5p^6$ for Ir) are treated as valence electrons, while with the ECP1-type basis, they are treated as part of the pseudopotential. The split valence form of Huzinaga's fully contracted all-electron basis sets[12] were used for all non-hydrogen ligand atoms; Huzinaga's (33/3) basis sets for carbon, nitrogen, and oxygen were split to (321/21), and the (333/33) sets for phosphorus and chlorine were split to (3321/321). The basis set for hydrogen was the (21) contraction of an STO-3G representation.[13] Pseudopotential basis sets were employed for the ligand atoms in the post-HFR calculations and were those due to Stevens et al.[14] All valence functions for the pseudopotential basis sets, except for the 5s function of the iridium ECP2 basis set, were split to form double-ζ contractions.

The optimizations were considered converged when the maximum gradient and the average gradient were less than 0.00075 and 0.0005 Hartree/au (or Hartree/radian), respectively. Multireference configuration interaction calculations with all single and double excitations to all virtual orbitals from the reference configurations (MRSDCI)[15] were applied to the HFR-optimized geometries. The reference configurations were generated as follows. The canonical HFR orbitals were generated from a calculation which employed pseudopotential basis sets on the ligand as well as the metal atoms. The valence orbitals from this calculation were localized according to the Boys' criterion,[16] from which GVB pairs[17] were constructed for the electrons involved in the bond-breaking/bond-forming process. This included the electrons in the H_2 σ_g orbital and those in the metal d_{xz} lone pair orbital in the plane of H_2 addition (assuming that H_2 adds along the z-axis). The 19 configurations generated from this four-electron four-orbital active space of the two GVB pairs constituted the reference configurations for the smaller of the two MRSDCI calculations. The larger MRSDCI calculations employed as reference configurations all 141 configurations generated from a six-electron six-orbital active space of three GVB pairs. The third pair corresponded to the metal d_{yz} lone pair electrons in the plane perpendicular to the plane of H_2 addition.

The GVB natural orbitals used to generate the configurations for the MRSDCI calculations were obtained after only 11 cycles of the GVB procedure. These calculations were not allowed to proceed to convergence since the converged GVB pairs did not correspond to the GVB pairs which initiated the calculation; the lone pair orbitals were no longer part of the active space. It is not uncommon for MCSCF procedures with small active spaces to find lower energy solutions by correlating the motion of electrons in other bonding orbitals rather than those in the lone pair orbitals of interest. The 11 cycles of the GVB calculation were sufficient to construct well-defined pairs from the initial set of occupied orbitals without allowing the orbital mixing to evolve the lone pair metal orbitals out of the active space.

All of the procedures mentioned above were performed from the GAMESS package of programs.[18] The topological analysis of the total charge density was performed through the application of Bader's theory of atoms in molecules,[19] which has been incorporated into the interactive version of MOPLOT.[20]

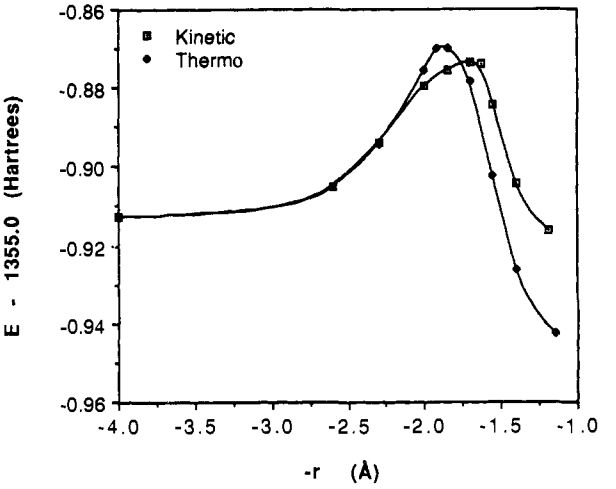

Figure 1. Reaction coordinate for the oxidative addition of H_2 to *cis*-$IrCl(CO)(PH_3)_2$. The point at r = 4.0 Å corresponds to the summation of the total energies from independent optimization calculations on H_2 and the square-planar metal complex (HFR calculations).

Results and Discussion

The reaction coordinate for the oxidative addition of H_2 to square-planar $IrCl(CO)(PH_3)_2$ along the two perpendicular ligand axes is shown in Figure 1. Addition along the P–Ir–Cl axis leads

(9) (a) Hay, P. J.; Wadt, W. R. *J. Chem. Phys.* **1985**, *82*, 299. (b) Hay, P. J.; Wadt, W. R. *J. Chem. Phys.* 270.
(10) Sargent, A. L.; Hall, M. B. *J. Comput. Chem.* **1991**, *12*, 923.
(11) Sargent, A. L.; Hall, M. B. *Topics in Physical Organometallic Chemistry*; M. Gielen, Ed., Vol. 4, in press.
(12) Huzinaga, S.; Andzelm, J.; Klobukowski, M.; Radzio-Andzelm, E.; Sakai, Y.; Tatewaki, H. *Gaussian Basis Sets for Molecular Calculations*; Elsevier: New York, 1984.
(13) Hehre, W. J.; Stewart, R. F.; Pople, J. A. *J. Chem. Phys.* **1969**, *51*, 2657.
(14) Stevens, W. J.; Basch, H.; Krauss, M. *J. Chem. Phys.* **1984**, *81*, 6026.
(15) (a) Siegbahn, P. E. M. *J. Chem. Phys.* **1980**, *72*, 1467. (b) Saunders, V. R.; van Lenthe, J. H. *Mol. Phys.* **1983**, *48*, 923.
(16) Foster, J. M.; Boys, S. F. *Rev. Mod. Phys.* **1960**, *32*, 300.
(17) Bobrowicz, F. W.; Goddard, W. A. *Methods of Electron Structure Theory*; Schaefer, H. F., Ed.; Plenum: New York, 1977.
(18) Guest, M. F. GAMESS; S.E.R.C. Daresbury Laboratory, Warrington WA4 4AD, U.K., 1990.
(19) (a) Bader, R. F. W. *Atoms in Molecules: A Quantum Theory*; Oxford University Press: Oxford, 1990. (b) Bader, R. F. W.; Essen, H. *J. Chem. Phys.* **1984**, *80*, 1943. (c) Bader, R. F. W.; MacDougall, P. J.; Lau, C. D. H. *J. Am. Chem. Soc.* **1984**, *106*, 1594.
(20) Interactive MOPLOT: a package for the interactive display and analysis of molecular wave functions incorporating the programs MOPLOT (Lichtenberger, D.), PLOTDEN (Bader, R. F. W.; Kenworthy, D. J.; Beddal, P. M.; Runtz, G. R.; Anderson, S. G.), SCHUSS (Bader, R. F. W.; Runtz, G. R.; Anderson, S. G.; Biegler-Koenig, F. W.), and EXTREM (Bader, R. F. W.; Biegler-Koenig, F. W.) Sherwood, P.; MacDougall, P. J. **1989**.

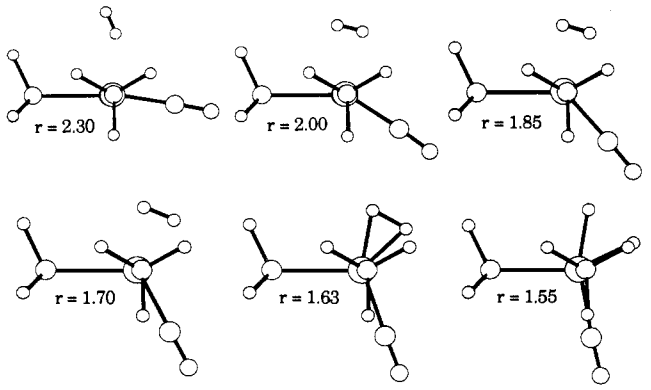

Figure 2. Optimized molecular geometries at six points along the reaction coordinate leading to the formation of the kinetic isomer.

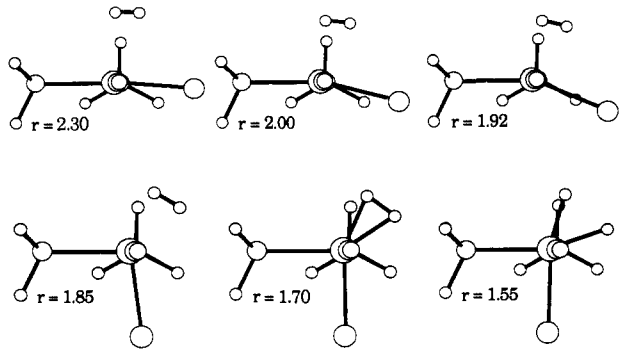

Figure 3. Optimized molecular geometries at six points along the reaction coordinate leading to the formation of the thermodynamic isomer.

to the formation of the more stable "thermodynamic" isomer, while addition along the P–Ir–CO axis leads to the formation of the "kinetic" isomer observed in high yield at low temperatures. The relative stabilities of the transition states and final products of the two isomers as predicted by the theory are in qualitative agreement with experiment. The optimized geometries at several points along the reaction coordinates leading to the formation of the kinetic and thermodynamic isomers are shown in Figures 2 and 3, respectively, and the optimized variables and total energies are reported elsewhere.[11] Notice that, in contrast to the smooth geometric evolution of the kinetic isomer, the evolution of the geometry for the thermodynamic isomer appears more discontinuous. The small change in r between 1.92 and 1.85 Å is accompanied by a nearly 60° change in α. Previous studies have pointed out that such apparent discontinuities are due to deviations of the chosen reaction coordinate from the true reaction coordinate.[21] Methods which are based on Fukui's intrinsic reaction coordinate have been developed to yield very good approximations of the true reaction coordinate.[21,22] However, the computational demands of these methods render them impractical for reactions involving a transition-metal complex as large as this one.

To obtain a more accurate description of the dependence of the true reaction pathway on r and α, we calculated the potential energy surfaces for both isomers in the vicinity of the transition states as a function of these two geometric parameters. All other geometric parameters described by model **1** were allowed to optimize. The potential energy surfaces are shown in Figures 4 and 5. The previous reaction coordinate denoted by the dashed line on the surfaces, closely follows the path of steepest descent from the saddle point for the kinetic isomer but not for the thermodynamic isomer. In the former case, α changes very little in the vicinity of the transition state; α maintains an intermediate value between the 0° and 90° extremes over a 0.20 Å change in r. In the latter case, the path of steepest descent from the saddle point

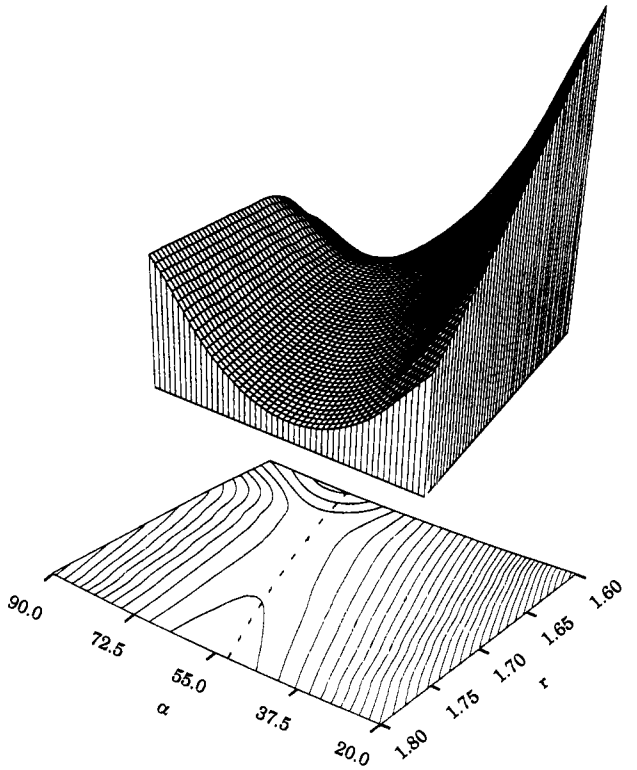

Figure 4. Potential energy surface in the vicinity of the transition state on the reaction path leading to the formation of the kinetic isomer. The dashed line corresponds to the pathway of the reaction coordinate r (see Figure 1). The contours are linear, differing by 0.001 hartree, with the lowest contour equal to −1355.876 hartree (HFR calculations).

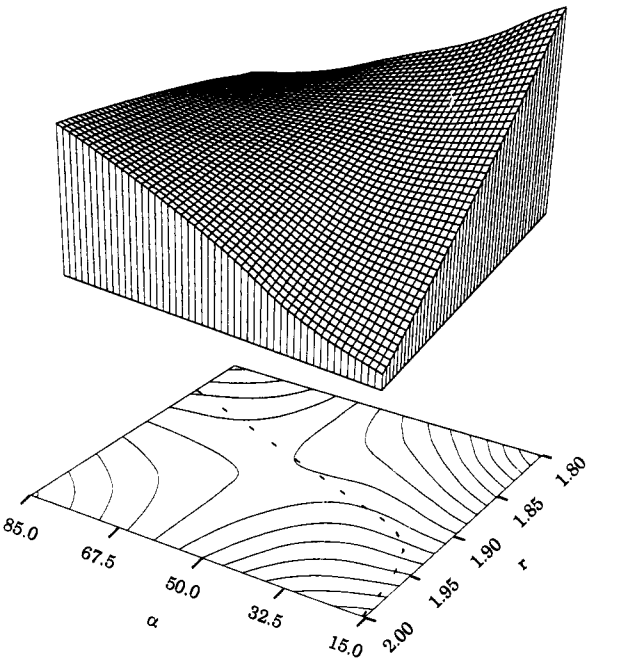

Figure 5. Potential energy surface in the vicinity of the transition state on the reaction path leading to the formation of the thermodynamic isomer. The dashed line corresponds to the pathway of the reaction coordinate r (see Figure 1). The contours are linear, differing by 0.001 hartree, with the lowest contour equal to −1355.875 hartree (HFR calculations).

corresponds to a large change in α over the same change in r. This large change in α which occurs in the vicinity of the transition state implies a strong correlation between the movement of the Cl ligand out of the plane of the square-planar complex and the barrier height.

(21) Ishida, K.; Morokuma, K.; Komornicki, A. *J. Chem. Phys.* **1977**, *66*, 53.
(22) Fukui, K.; Kato, S.; Fujimoto, H. *J. Am. Chem. Soc.* **1975**, *97*, 1.

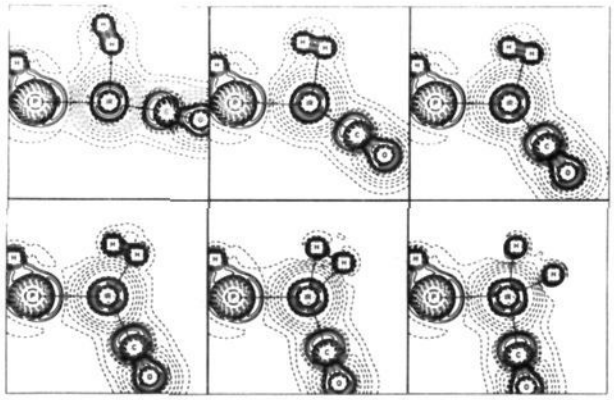

Figure 6. Plots of $-\nabla^2\rho$ for six points along the reaction pathway leading to the formation of the kinetic isomer. These are the same six points shown in Figure 2. Ten geometric contours of each sign are plotted. The absolute value of the smallest contour is 0.03906 e/a_0^5.

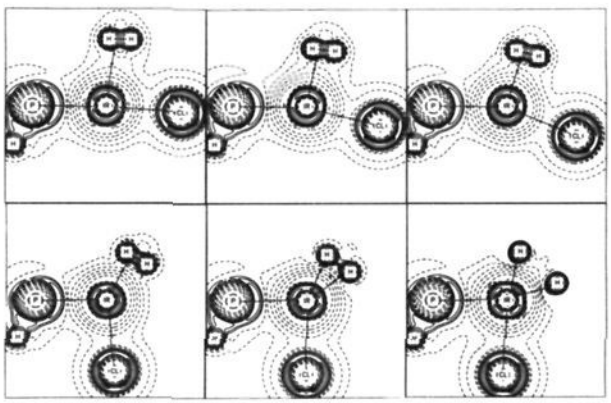

Figure 7. Plots of $-\nabla^2\rho$ for six points along the reaction pathway leading to the formation of the thermodynamic isomer. These are the same six points shown in Figure 3. The plots were contoured as in Figure 6.

What causes this difference in the coupling between α and r near the transition states leading to the formation of the two isomers? Stated differently, why is the CO ligand so willing to bend out of the plane of the square-planar complex in the early stages of the reaction, while the Cl ligand resists this motion until it is closer to the transition state? The results from the qualitative theoretical studies[3] provide a clue. The backbonding interaction between the filled metal d_{z^2} orbital and the unoccupied CO $2\pi^*$ orbital, as H_2 adds in the P–M–CO plane, provides additional stabilization to the five-coordinate species, as shown in **2**. If, however, H_2 adds in the plane of the Cl ligand, which is a π-donor ligand, the corresponding orbital interaction, **3**, is antibonding and destabilizing. These model interactions are greatly simplified

2 **3**

from the actual orbital interactions which involve substantial orbital mixing as the reaction proceeds under the low symmetry (C_1) conditions. In order to analyze the difference between the reaction pathways without recourse to a particular orbital model, we analyzed the topology of the total charge density.[19]

The plots of the negative of the Laplacian of the total charge density, $-\nabla^2\rho$, shown in Figures 6 and 7, display regions of charge concentration ($-\nabla^2\rho > 0$, denoted by solid contours) and charge depletion ($-\nabla^2\rho < 0$, denoted by dashed contours). Overlaid on these plots are the bond paths and critical points, which are collectively referred to as the molecular graph.[19] The bond paths trace the paths of maximum charge density between two nuclei, while the bond critical points denote the one-dimensional minimum of charge along these paths and the two-dimensional maximum normal to the paths.

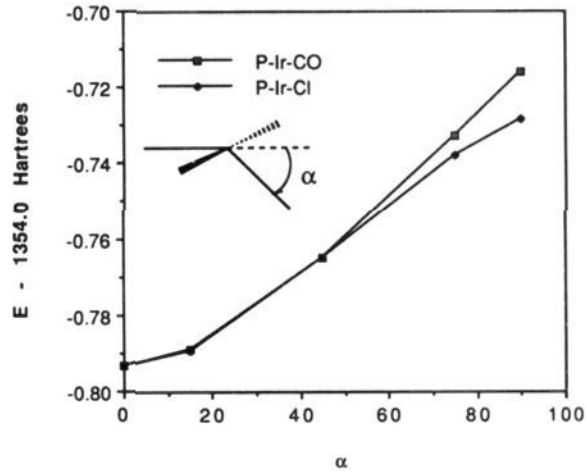

Figure 8. Total energy as a function of the bending angle α for bending the two perpendicular ligand axes of the square-planar complex in the absence of H_2. All bond distances were optimized for each point in the curve.

The plots in Figures 6 and 7, for $r = 2.3$ Å, illustrate that there are regions of charge concentration above and below the square-planar complex. The concentrations are due, in part, to the electrons in the lone pair 5d metal orbitals; the 5s and 5p electrons also contribute to these concentrations.[23] As the complex evolves from a four-coordinate to a six-coordinate species, the ligands in the plane of addition must move past these regions of charge accumulation. The CO ligand, with low-energy unoccupied orbitals, can accept electron density from the concentrations of charge around the metal center as it passes through these regions and thereby reduce the repulsive interaction between its own electron density (mainly 5σ density) and that on the metal center. An additional repulsive interaction between the electron density around the metal center and that of the approaching H_2 unit can also be decreased through the electron-withdrawing facet of the CO ligand when addition occurs in this plane. Notice, in Figures 4 and 6, the intermediate values of α that are maintained throughout a large portion of the reaction coordinate.

The Cl^- ligand is purely an electron-donor ligand. The interaction between the metal and Cl^- for intermediate values of α is repulsive as concentrations of charge pass within close proximity to each other. Movement of the Cl^- ligand past the concentrations of charge at the metal center corresponds to the movement along the reaction coordinate through the saddle point. Other ligands, most notably strong σ-donors such as hydride, elicit the same behavior in the vicinity of the transition state if they replace the chloride ligand in the square-planar complex.[11]

It is important to realize that bending the P–Ir–Cl ligand axis out of the plane of the square-planar complex in the absence of H_2 is easier than bending the P–Ir–CO ligand axis. Figure 8 illustrates that there is very little difference in energy between bending the P–Ir–Cl and P–Ir–CO axes up until an angle of about 50°, after which bending the former requires less energy. This difference seems to be controlled by the HOMO, which, in this d^8 complex, is M–L σ antibonding with respect to the ligands which are bending.[11] The weaker M–Cl bond has less to lose

(23) The regions of charge concentration around the metal center are actually saddle points in the plane of addition, rather than local maxima; the local maxima reside in and out of the plane of addition. The difference in magnitude between concentrations at the saddle point and at the maxima are small in this case.

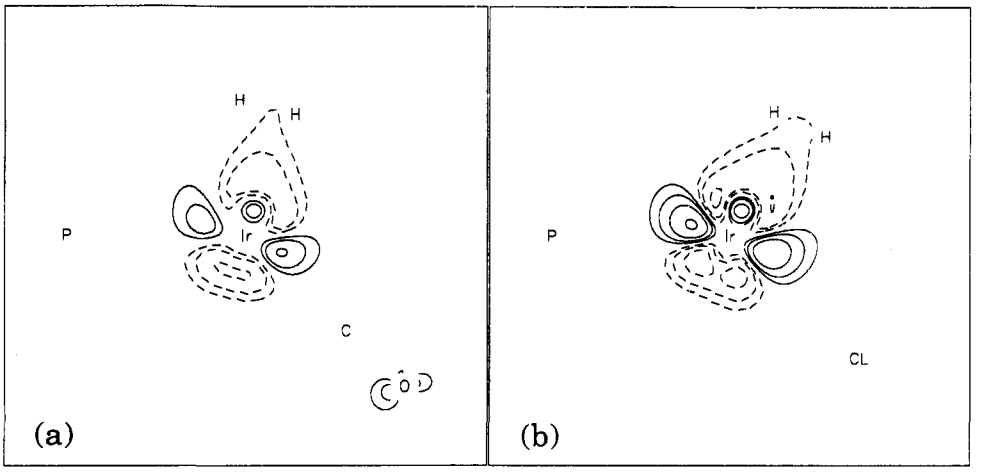

Figure 9. Deformation density in the plane of addition with H_2 adding in the (a) P–Ir–CO and (b) P–Ir–Cl planes in $IrCl(CO)(PH_3)_2$. The structure was optimized with α fixed at 45° and r fixed at 1.885 Å. Promolecule densities for H_2 and $IrCl(CO)(PH_3)_2$ were subtracted from the total density of $IrH_2Cl(CO)(PH_3)_2$. The contours are geometric, differing by a factor of 2, with the value of the smallest positive and negative contour equal to ± 0.00781 e/a_0^3. Negative contours are dashed.

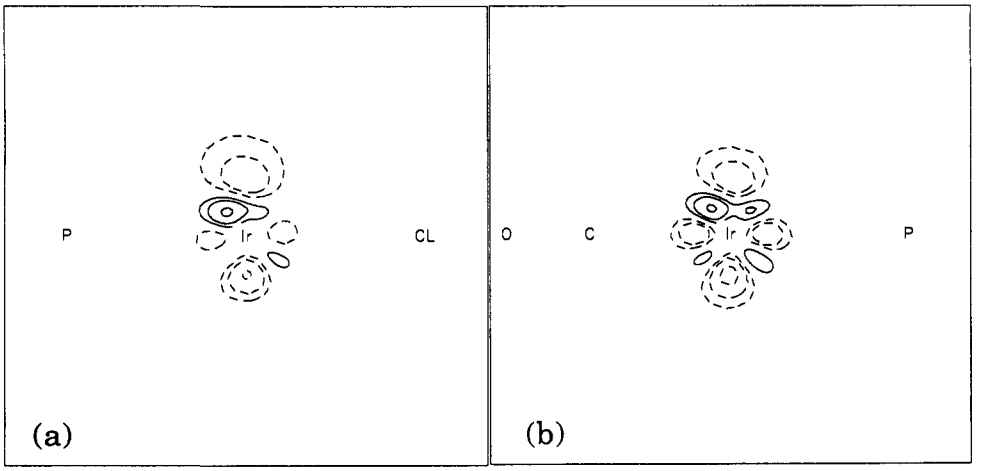

Figure 10. Deformation densities in planes that are perpendicular to the corresponding planes of addition plotted in Figure 9. Densities are contoured as in Figure 9.

energetically by this occupied antibonding interaction than does the stronger M–CO bond. Hence, for large α ($50° < \alpha \leq 90°$), the four-coordinate complex in which the P–Ir–Cl axis is bent is lower energy than that in which the P–Ir–CO axis is bent.

The deformation density plots, shown in Figures 9 and 10, display the difference between the total molecular density of $IrH_2Cl(CO)(PH_3)_2$ and the H_2 and $IrCl(CO)(PH_3)_2$ fragment (or promolecule) densities. These plots illustrate that the approach of the H_2 unit polarizes electron density into regions of the adjacent metal–ligand bonds in the plane of addition. How well these adjacent ligands can accommodate the additional charge density around the iridium center as the complex evolves from a four-coordinate to a six-coordinate species distinguishes between the two pathways to addition. In the case where H_2 adds in the P–Ir–CO plane, the accumulation of density on the carbonyl oxygen atom, shown in Figure 9a, indicates that this ligand delocalizes some of the density from the metal center that is polarized due to the approaching H_2 ligand.

Eisenberg and co-workers recently reported that at low H_2 pressures, an alternative to the reductive elimination/oxidative addition mechanism for the isomerization of the kinetic to the thermodynamic isomer exists.[24] This mechanism involves the bimolecular dihydride transfer directly from the kinetic isomer to the square-planar complex along the P–Ir–Cl axis to form the thermodynamic isomer. These results suggest that in the absence of the H_2 σ_g bonding electron density, the oxidative addition of "H_2" to $IrCl(CO)(PH_3)_2$ will proceed directly along the thermodynamic pathway; that is, "H_2" addition along the P–Ir–Cl axis will be lower than that along the P–Ir–CO axis. Our calculations support this concept; the addition of H_2 with a fixed bond distance of 2.1 Å (corresponding to the distance between the two hydrides in the six-coordinate final products) to the square-planar complex is lower in energy for the addition along the P–Ir–Cl axis at all points along the reaction coordinate. The lack of concentrated electron density in the coordination site of the H_2 unit in the five-coordinate transition state allows for the polarization of the nonbonding charge density around the metal center into this space. The energetics of the addition reaction along the two pathways will then resemble that illustrated in Figure 8.

Finally, the effects of electron correlation on our reaction coordinate were examined, and the results are presented in Figure 11. The calculations involving all single and double excitations out of 19 reference configurations, yielding a 20 306 configuration CI wave function, are shown in the middle set of curves in Figure 11. The relative stabilities of the transition states and the final products for both pathways of addition remain unaltered from the HFR results. The positions of the transition states relative to the reaction coordinate, however, have become more reactant-like with the inclusion of electron correlation. The relative energetic gains of correlating the motion of the electrons involved in the bond-breaking/bond-forming process are higher the closer these electrons are to each other; this accounts for the shift of the transition states to the left and indicates that the inclusion of the correlation energy yields a reaction which is more exothermic.

(24) Kunin, A. J.; Johnson, C. E.; Maguire, J. A.; Jones, W. D.; Eisenberg, R. *J. Am. Chem. Soc.* **1987**, *109*, 2963.
(25) Sargent, A. L.; Hall, M. B. *Inorg. Chem.*, in press.

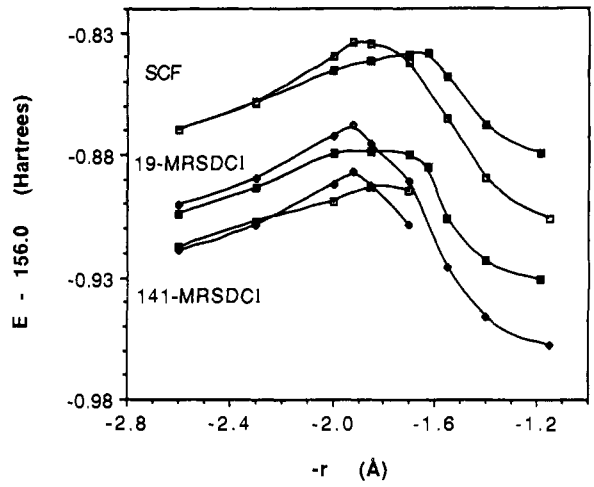

Figure 11. Reaction coordinate for the oxidative addition of H_2 to *cis*-$IrCl(CO)(PH_3)_2$ calculated with core potential basis sets on all non-hydrogen atoms and (a) a single-determinant HFR wave function, (b) a MRSDCI wave function with 19 reference configurations, and (c) a MRSDCI wave function with 141 reference configurations. All calculations were performed at the optimized HFR geometries.

The difference in the energies between the two reaction paths at large values of r for the middle set of curves in Figure 11 seem to indicate that there is an early preference for H_2 addition along the P–Ir–CO axis. This result is not physically meaningful but is, instead, an artifact of the calculation. The "lone pair" metal orbital in the P–Ir–CO plane contains substantial CO ligand character, while the corresponding orbital in the P–Ir–Cl plane contains little ligand character. The contribution of the back-bonding interaction between the metal "lone pair" orbital and the CO $2\pi^*$ orbital stabilizes the addition reaction in the P–Ir–CO plane relative to that in the P–Ir–Cl plane to a large extent in the CI calculation and renders the comparison between the two pathways invalid for large r. When the electrons in the lone pair orbitals in both planes are included in the CI calculations (i.e., all metal d electrons), this early preference disappears, as shown in the lowest set of curves in Figure 11. The errors in the early part of the curves for the 19-MRSDCI calculations were not carried through to the remainder of the curves, and the conclusions drawn from the latter portions of the curves are supported by the 141-MRSDCI calculations. These last calculations utilized a total 252 175 configurations, generated from all single and double excitations out of 141 reference configurations (vide supra).

Conclusion

The difference in the barrier heights to the addition of H_2 along the P–Ir–CO and P–Ir–Cl axes is due to the difference in how the ligands in the plane of addition accommodate the electron–electron repulsive interactions due to the close encounter of these ligands with the charge concentrations on the metal center as the complex evolves from a four-coordinate to a six-coordinate species. Since one phosphine ligand is present in both planes of addition, the effects of these ligands essentially cancel, and the comparison is simplified to one between the CO and Cl ligands. The similarity in size between CO and Cl eliminates steric influences and further simplifies the comparison to their electronic differences. Addition in the P–Ir–CO plane is favored due to the electron-withdrawing nature of the CO ligand. The interelectronic repulsions between the concentrations of charge around the metal atom and the electron density of the ligands in the plane of addition are reduced through the delocalization of some of this charge at the metal center by the low-energy unoccupied CO $2\pi^*$ orbitals. In the vicinity of the transition state, the CO ligand moves very little as the H_2 unit approaches and maintains an orientation aligned with the concentration of charge at the metal center. The Cl ligand is unable to reduce these repulsions when H_2 adds in the P–Ir–Cl plane. In the vicinity of the transition state, the movement of the Cl ligand is large and indicates that the interactions between the ligand and the charge around the metal center are purely repulsive. The inclusion of electron correlation did not significantly alter the results obtained from the HFR wave functions.

When H_2 adds to d^8 square-planar complexes with a trans orientation of the phosphine ligands, the direction of addition will be determined by comparing how well the pairs of ligands in the two planes accommodate the concentrations of charge around the metal center in the five-coordinate stage of the reaction. Results from studies of the oxidative addition of H_2 to *trans*-$IrX(CO)(PR_3)_2$ (X = H, Cl, CH_3, C_6H_5; R = H, CH_3) are reported elsewhere.[11,25]

Acknowledgment. The authors thank the Robert A. Welch Foundation (Grant No. A-648) and the National Science Foundation (Grant No. CHE 86-19420) for their support. A.L.S. thanks the Shell Foundation for a predoctoral fellowship. This research was conducted in part using the Cornell National Supercomputer Facility, a resource of the Center for Theory and Simulation in Science and Engineering at Cornell University, which is funded in part by the National Science Foundation, New York State, and the IBM Corporation. We also thank the Engineering Resources Center at Texas A&M University for a grant of computer time on the CRAY Y-MP2/116.

Registry No. IrCl(CO)(dppe), 87985-29-3; H_2, 1333-74-0.

Supplementary Material Available: Tables I and II of the optimized geometric parameters and total energies for the nine values of r along with the reaction coordinates leading to the kinetic and thermodynamic isomers, respectively (2 pages). Ordering information is given on any current masthead page.